Biofilm 11 (2026) 100370

Contents lists available at ScienceDirect

Biofilm

journal homepage: www.sciencedirect.com/journal/biofilm

Evidence of cefiderocol-persistence in *Pseudomonas aeruginosa in vitro* biofilms and in a murine infection model

Gianmarco Mangiaterra [a,*], Massimiliano Lucidi [b], Giorgia Piccioni [a], Riccardo Rosa [a], Davide Gugliandolo [c], Ida De Fino [c], Martina Rossano [c], Carla Vignaroli [d], Paolo Visca [b], Alessandra Bragonzi [c], Barbara Citterio [a]

[a] *Department of Biomolecular Sciences, University of Urbino Carlo Bo, Biotechnology Section, Fano, 61032, Italy*
[b] *Department of Science, University Roma Tre, Rome, 00154, Italy*
[c] *Infections and Cystic Fibrosis Unit, Division of Immunology, Transplantation and Infectious Diseases, IRCCS San Raffaele Scientific Institute, Milan, 20132, Italy*
[d] *Department of Life and Environmental Sciences, Polytechnic University of Marche, Ancona, 60131, Italy*

ARTICLE INFO

Keywords:
Pseudomonas aeruginosa
VBNC cells
Antibiotic persistence
Cystic fibrosis
Chronic infections

ABSTRACT

Background: Persistent and viable but non-culturable (VBNC) *Pseudomonas aeruginosa* cells hamper the eradication and contribute to the recurrence of biofilm-related infections, especially in cystic fibrosis (CF) patients, often experiencing difficult-to-treat lung infections. The siderophore-cephalosporin cefiderocol, which hijacks bacterial iron-uptake systems, has emerged as a last-resort antibiotic against antibiotic-resistant Gram-negative bacteria and represents a desirable therapeutic option; however, there is still limited information about its impact on bacterial persisters.

Methods: P. aeruginosa biofilms were exposed to either tobramycin, ceftazidime, or cefiderocol at their minimum biofilm eradication concentrations under iron depletion in a rich or minimal medium. The bacterial survivors were quantified by combining cultural enumerations, quantitative PCR and confocal microscopy, to detect both culturable and VBNC cells. To extend these observations *in vivo*, a murine model of *P. aeruginosa* lung infection was employed, and bacterial burden and VBNC frequency were assessed following antibiotic treatment.

Results: A higher amount of culturable *P. aeruginosa* cells was recovered after cefiderocol challenge (~10^5 CFU/ml) compared to tobramycin and ceftazidime (10^3-10^4 CFU/ml). Notably, it induced a significantly lower proportion of VBNC cells (~85.2%) than the aminoglycoside (98.95%) or ceftazidime (95.80%).

Consistently, cefiderocol exposure resulted in a higher bacterial survival *in vivo*, but in a lower frequency of VBNC subpopulation (71.89%) compared to tobramycin (81,58%).

Conclusions: Overall, these findings emphasize the capacity of *P. aeruginosa* to withstand treatment with cefiderocol and highlight the need to account for the roles of bacterial persisters and VBNC cells in the recurrence of chronic infections, particularly among CF patients.

1. Introduction

Pseudomonas aeruginosa is a Gram-negative ubiquitous species, widespread in soil, water and within various plant and animal hosts [1]. Its versatility is the result of extreme adaptability, due to fine gene expression regulation, strong genome plasticity [2], and a high number of regulatory sequences in the bacterial chromosome [3].

In humans, *P. aeruginosa* acts as an opportunistic pathogen, responsible for infections in immunocompromised or traumatized subjects, such as those hospitalized in intensive care units [4], those suffering from deep wounds and burns, or those with catheters [1]. It is considered the main and most dangerous bacterial pathogen for Cystic Fibrosis (CF) patients, who suffer from recurrent, often chronic, and difficult-to-treat infections [5]. Although *P. aeruginosa* is not among the first bacterial colonizers of the CF lungs, it eventually outcompetes other pathogens due to its remarkable ability to adapt to the lung environment [6] and to produce a thick and structured biofilm. Within the biofilm matrix, *P. aeruginosa* cells are protected from the activity of the immune system and antibiotic pressure, managing to survive and to proliferate [7]. Persistent colonization with *P. aeruginosa* has been observed even in

* Corresponding author. via Arco d'Augusto n.2, 61032, Fano, (PU, Italy.
E-mail address: gianmarco.mangiaterra@uniurb.it (G. Mangiaterra).

https://doi.org/10.1016/j.bioflm.2026.100370
Received 28 February 2026; Received in revised form 28 April 2026; Accepted 28 May 2026
Available online 28 May 2026

CF patients receiving Cystic Fibrosis Transmembrane Conductance Regulator (CFTR) modulator therapies [8].

Biofilms constitute complex bacterial communities composed of distinct niches, each characterized by specific environmental conditions (*e.g.,* salinity, pH, oxygen levels) that influence bacterial growth and behavior [9]. This structural heterogeneity can promote the emergence of specialized phenotypes that are better adapted to such environmental conditions. A typical example is represented by the mucoid phenotype, considered a hallmark of chronic CF infection, which arises from alginate hyperproduction [10]. Other specialized cell variants found in both planktonic and biofilm lifestyles are persisters and Viable but Non-Culturable (VBNC) cells. Persisters are defined as a subpopulation of bacteria that survive under stressful conditions, including antibiotic treatment, by entering a transient quiescent state by slowing the metabolism [11]. Upon stress removal, these dormant cells can resume full metabolic activity and return to an actively replicating state. VBNC cells represent a deeper state of dormancy [12], where cells completely lose the ability to form colonies on solid media even when the stress condition is ceased. Such quiescent forms escape routine culture-based microbiological diagnosis [13] but can regain culturability through a process known as 'resuscitation,' which occurs once stress is relieved, and specific factors stimulate bacterial metabolism [12]. Such features clearly indicate the involvement of both persisters and VBNC cells in the failure of eradication of biofilm-mediated infections caused by *P. aeruginosa*. It has been shown that *P. aeruginosa* VBNC cells occur in CF sputum samples and can be induced by antibiotic treatment [13,14]. Indeed, exposure to tobramycin (TOB), which is considered the gold standard treatment for *P. aeruginosa* lung infections [15], induces the transition of cells into the VBNC state, and antibiotic efflux is the key driver of the conversion of vegetative cells into dormant ones [16]. This work is aimed to evaluate the involvement of cefiderocol (CFD), a recently developed antibiotic representing an emerging 'last-resort' option for multidrug-resistant (MDR) infections [17], in the development of these dormant cells. CFD consists of the modification of a cephalosporin scaffold by adding a chlorocatechol moiety, which enables the drug to bind iron and to act as a siderophore [18]. Iron starvation has been long considered as an effective antimicrobial strategy, and some iron chelators have shown promising antibacterial activity [19]. In this context, CFD plays a Trojan horse strategy, designed to induce the active uptake of the antibiotic, which can reach its target (*i.e.,* the bacterial cell wall) and exert its antibacterial activity. Moreover, the CFD molecule was designed to reduce its susceptibility to β-lactamase activity and to have a poor affinity for efflux pumps [20], making this antibiotic a desirable therapeutic option even in CF [21]. However, some reports have already shown the emergence of CFD-resistant *P. aeruginosa* strains [22,23], as well as the formation of planktonic persister cells following CFD treatment [24]. Here, we demonstrate the persistence of *P. aeruginosa* biofilms when exposed to Minimum Biofilm Eradication Concentrations (MBECs) of CFD and analyzed the induction of VBNC subpopulations after antibiotic treatment, in comparison with suitable anti-pseudomonal drugs, such as the cephalosporin ceftazidime (CAZ) and TOB. These findings were further validated in a preclinical murine model of *P. aeruginosa* lung infection.

2. Materials and methods

2.1. Bacterial strains, culture media and chemicals

The *P. aeruginosa* strains used in this study are ATCC 27853, PAO1, and the iron biosensor PAO1 P*pvdE::lux*, where the expression of the *lux* operon is driven by the promoter of the pyoverdine biosynthetic gene *pvdE* [25]. Bacterial strains were cultured in cation-adjusted Mueller--Hinton broth (MHII), its iron-depleted variant (ID-MHII), and in the minimal medium M9 supplemented with succinate 20 mM as carbon source, and conserved as glycerol stocks (20%) in MHII broth at −80 °C. For ID-MHII preparation, the MHII broth was treated with 10% Chelex 100 resin (Bio-Rad Laboratories, Milan, Italy) and supplemented with $MgSO_4$ 11.25 μg/ml, $CaCl_2$ 22.5 μg/ml, and $ZnSO_4$ 1 μg/ml according to the CLSI guidelines [26]. M9 broth was prepared in iron-limiting conditions, *i.e.,* using acid-washed glassware, plasticware, and iron-limited reagents, and sterilized by filtration (0.22 μm). All antibiotics were purchased by Merck (Merck KGaA, Darmstadt, Germany).

2.2. Growth curve analysis, iron-depletion sensing and biofilm formation

The stress caused by iron depletion on *P. aeruginosa* growth was investigated by growth curve analysis. The *P. aeruginosa* strains PAO1 and PAO1 P*pvdE::lux* were cultured overnight in MHII, ID-MHII, or M9, washed with sterile iron-limited saline, and diluted in each medium at a final optical density at 600 nm (OD_{600nm}) of 0.01. Bacterial growth was monitored hourly at 37 °C for 24h, measuring the OD_{600} using the Spark 10 M microplate reader (Tecan Spark, Tecan Trading AG, Switzerland). To provide evidence of iron depletion, the luminescence emitted by *P. aeruginosa* PAO1 P*pvdE::lux* was measured in each medium at the end of the exponential growth phase (*i.e.,* after 10 h) and normalized by the corresponding OD_{600}.

P. aeruginosa PAO1 ability to form biofilm was evaluated using the crystal violet assay. Briefly, bacterial suspensions ($OD_{600} = 0.1$) in each medium were inoculated in 96-well flat-bottom plates and incubated for 24 h at 37 °C. After washing with sterile iron-limited saline, biofilms were stained with 1% (w/v) crystal violet for 15 min and then washed again. The crystal violet-stained biofilm was then dissolved in 96% (v/v) ethanol, and the optical density at 570 nm (OD_{570}) was measured. The obtained values were normalized by the corresponding OD_{600}.

All assays were performed in technical triplicate and biological duplicates.

2.3. Antibiotic susceptibility assays

P. aeruginosa susceptibility to CFD, TOB, and CAZ was assessed by determining the antibiotic minimum inhibitory concentrations (MICs) by broth microdilution in ID-MHII and M9, according to CLSI guidelines [26]. Moreover, the antibiotic MBECs were determined in both ID-MHII and M9 using the Calgary biofilm device (Innovotech Inc., Edmonton, Canada), according to Revest et al. [27].

All assays were performed at least twice.

2.4. Antibiotic persistence assays in planktonic cultures

Antibiotic persistence was assessed in *P. aeruginosa* PAO1 cultures in both ID-MHII and M9, exposed to CFD, TOB or CAZ. Briefly, overnight cultures were diluted and refreshed in each medium and incubated at 37 °C in shaking (200 rpm) till reaching the end of the exponential growth phase ($OD_{600} = 0.6$). The cultures when then exposed to 20xMICs of each antibiotic for 24 h, and the amount of *P. aeruginosa* persisters was evaluated after 0, 1, and 24 h exposure. The typical biphasic killing pattern was verified in preliminary experiments to select these specific exposure times. At each time point, 1 ml-aliquots of the cultures were centrifuged 3300 rpm for 5 min, resuspended in 1 ml of antibiotic-free fresh medium and quantified by viable plate counts performed on MH agar plates. Bacterial counts were evaluated till 72h incubation at 37 °C.

All assays were performed two times in biological duplicates.

2.5. P. aeruginosa biofilm model and antibiotic persisters quantification

P. aeruginosa PAO1 biofilms were developed in 24-well flat-bottom plates, each well containing round (13 mm diameter) polyethylene terephthalate coverslips. *P. aeruginosa* suspensions in ID-MHII or M9 ($OD_{600} = 0.1$) were inoculated into each well and incubated at 37 °C for 24 h; then, the produced biofilms were washed three times with sterile iron-limited saline and challenged with ID-MHII or M9 containing CFD,

TOB, or CAZ at their MBEC for an additional 24 h at 37 °C. The biofilm carriage of culturable and VBNC *P. aeruginosa* cells was quantified upon formation and after exposure to the antibiotics. Briefly, biofilms were washed, and the coverslips were transferred into 2.5 ml of sterile iron-limited saline. Biofilm cells were detached by three cycles of mild sonication (60 s) followed by incubation on ice (60 s). Appropriate dilutions were then used to quantify the different persister populations: (*i*) culturable survivors were determined by serial 10-fold dilutions and plating on MH agar, incubated at 37 °C for 72 h; (*ii*) the VBNC subpopulation was estimated as the difference between *P. aeruginosa* total viable cells (TVCs) and culturable cells, with TVCs quantified by *ecfX*-qPCR using previously validated DNA extraction and amplification protocols designed to exclude extracellular DNA and dead cells [**14**]. The presence of a VBNC subpopulation was indicated by a threshold difference between TVCs and culturable persisters of 0.5 log. All assays were performed in technical triplicates and biological duplicates.

2.6. Biofilm formation in flow cells, confocal microscopy, and image analysis

Biofilm formation on a glass surface was investigated in a flow cell system, as previously described [28]. Briefly, an overnight culture of *P. aeruginosa* PAO1 was diluted to an OD_{600} of 0.2 in M9 and inoculated in the biofilm flow chambers (Ibidi). Flow chambers were incubated for 2 h at 37 °C to facilitate bacterial adhesion. Then, a flow of M9 at a rate of ~150 μl/min was streamed into the flow chambers. Following incubation at 37 °C for 24 h, biofilms were treated with 256 μg/ml CFD, 1024 μg/ml CAZ, and 16 μg/ml TOB for another 24 h at 37 °C. Untreated biofilm, used as a control, was incubated in M9 for 24 h at 37 °C. Then, treated and untreated biofilms were stained with a combination of 10 μM SYTO 9, 5 mM 5-cyano-2,3-ditolyl tetrazolium chloride (CTC), and 2.5 μM kK 1905, or 0.1% (w/v) Acridine Orange (AO) for 30 min at 37 °C. In particular, SYTO 9 was used to stain all cells [29], KK 1905 to identify membrane-damaged cells [29], CTC to quantify respiratory activity [30], and AO to estimate RNA and DNA content [31]. The stained biofilms were imaged using the Nikon A1R + confocal laser-scanning microscope (CLSM) equipped with an Apo 40× objective. Laser lines at 488 nm, 561 nm, and 640 nm were used for SYTO 9, CTC, and KK 1905 excitation, respectively. Emission bandwidths of 490-550 nm, 600-640 nm, and 660-720 nm were employed to collect the fluorescence emission of SYTO 9, CTC, and KK 1905, respectively. Excitation lasers of 488 nm and 561 nm were used for DNA- and RNA-binding forms of AO. The emission bandwidths for DNA- and RNA-binding forms of AO were 500-550 nm and 600-720 nm, respectively. Multidimensional images were acquired at a sampling dimension of 1024×1024 pixels and processed (deconvolution and 3D rendering) with the NIS-Elements Confocal software (Nikon). Biofilm biomass and average thickness were determined using at least five image stacks employing COMSTAT v.2.1, as previously described [32]. Cell membrane integrity and respiratory activity were calculated according to the following equations:

$$\text{Cell membrane integrity} = \text{biomass}_{\text{SYTO 9}} / \text{biomass}_{\text{KK 1905}};$$

$$\text{Respiratory activity} = \text{biomass}_{\text{CTC}} / \text{biomass}_{\text{SYTO 9}}.$$

Since AO is a metachromatic dye that undergoes bathochromic shifts when binding DNA or RNA, emitting green or red fluorescence, respectively [33], the ratio between the biomass calculated for DNA- and RNA-dependent emissions was measured as a proxy of cell transcriptional activity in biofilms [31]. Cell area and aspect ratio were calculated using ImageJ v.1.53c (Fiji) for >1000 cells of each condition, as previously reported [34].

2.7. Mouse model of chronic P. aeruginosa infection

Animal studies adhered to the Italian Ministry of Health guidelines for the use and care of experimental animals (IACUC #1438). Immunocompetent C57BL/6NCrlBR male mice (8-10 weeks; Charles River Laboratories, Calco, Italy) were challenged with 1×10^6 colony-forming units (CFUs) of *P. aeruginosa* PAO1 strain embedded in agar beads for chronic infection by intratracheal administration, as previously described [35,36]. Twenty-four hours after infection, mice were treated with TOB 80 mg/kg, CFD 40 mg/kg, or vehicle (saline) by subcutaneous injection. The doses of antibiotics were chosen on the basis of their MICs. Body weight was monitored daily, lung CFUs and cell counts in the bronchoalveolar lavage fluid (BALF) were analyzed as previously described [37,38]. Twenty-five mg of homogenates were then used for total DNA extraction and qPCR assays to quantify *P. aeruginosa* TVC as described above.

Clearance was defined as the recovery of $<10^3$ total CFU following antibiotic treatment, while counts of $\geq 10^3$ CFU were considered indicative of persistent infection, as established previously [39]. Four-five mice for each condition (*i.e.*, treatment with saline, TOB, or CFD) were used in two independent experiments.

2.8. Statistical analysis

Each experimental procedure was performed at least two times. The statistical significance of the different *P. aeruginosa* VBNC cell abundances after antibiotic treatment and of the *P. aeruginosa* luminescence emission and biofilm production was assessed by Welch two-sample *t*-test, when a pairwise comparison was possible. For the pairwise multiple comparison, the non-parametric Kruskal-Wallis test and a Bonferroni corrected alpha of 0.017 was used. Statistical significance was considered for p values < 0.05. All *in vitro* analyses were carried out by R software version 4.5.1.

Specifically for *in vivo* tests, statistical analyses were performed with GraphPad Prism (GraphPad Software, Inc., San Diego, CA, USA) using a two-way ANOVA (Dunnett) test for body weight changes and one-way ANOVA (Dunnett) for the other readouts. Outlier data, identified by Grubbs' test, were excluded from the analysis.

3. Results

3.1. Iron depletion impacts P. aeruginosa growth and biofilm formation

Since the CLSI guidelines recommend the use of iron-depleted media to test CFD susceptibility [26], the *P. aeruginosa* PAO1 growth profile was preliminarily determined in iron-depleted cation-adjusted Mueller-Hinton broth (ID-MHII) and in the M9 minimal medium prepared in iron-limiting conditions and compared with the conventional MHII broth (Fig. S1A). Growth was strongly influenced by iron availability in the media, with differences evident as early as 8 h. Among the tested media, MHII supported the highest growth level, whereas ID-MHII and M9 resulted in reduced growth. Specifically, in M9 medium, growth was initially faster than in ID-MHII, but during the final phase of the experiment (20–24 h), the growth levels in the two media became comparable.

Iron depletion was confirmed using a previously developed *P. aeruginosa* biosensor strain [25], which emits luminescence in response to iron starvation (Fig. S1B). Both ID-MHII and M9 were sensed as iron-depleted media by *P. aeruginosa*, with a more evident effect in ID-MHII (6-fold increase in luminescence compared to MHII) than in M9 (3-fold increase compared to MHII). Biofilm production was assessed as well, showing that lower iron availability in ID-MHII resulted in a reduced ability to form biofilm (34% decrease) compared to MHII, whereas M9 induced a stronger biofilm production (311%) (Fig. S1C).

Finally, the susceptibility of *P. aeruginosa* PAO1 planktonic cultures and biofilms to CFD was assessed in both iron poor media (ID-MHII and M9) and compared with TOB and CAZ. Concerning the planktonic cultures, CFD exhibited the lowest (0.5 μg/ml) MIC among the three antibiotics (1 μg/ml for both TOB and CAZ). The culture medium did not

affect the bacterial susceptibility to the drugs. The MIC values of the reference strain *P. aeruginosa* ATCC 27853 matched the expected ranges reported in the CLSI guidelines [26], thus assuring the assay reliability. All the antibiotics were also endowed with a bactericidal effect at these concentrations. TOB was the most effective antibiotic on *P. aeruginosa* biofilms, exhibiting a MBEC of 16 μg/ml, followed by CFD (256 μg/ml) and CAZ (2048 μg/ml in ID-MHII and 1024 μg/ml in M9); even in this case, no significant differences were detected between the two culture media, since the only MBEC variation was ≤2 fold anyway.

3.2. *P. aeruginosa* CFD persisters in planktonic cultures

Late exponential growth-phase *P. aeruginosa* PAO1 cultures were exposed to bactericidal concentrations (*i.e.,* 20×MIC) of CAZ, CFD, and TOB. The number of *P. aeruginosa* CFU was monitored at 0, 1, and 24h after exposure (Fig. S2).

The strongest effect of antibiotic exposure was exhibited within the first hour, with a ~0.5 log decrease in CFU counts, irrespective of the used drug. TOB-exposed cultures showed further decreases after 24 h in both ID-MHII and M9. In contrast, CAZ and CFD caused only a slight decrease in M9, while in ID-MHII, the cultures adapted and maintained stable CFU values over time.

3.3. *P. aeruginosa* CFD persisters and VBNC cells in biofilms

Culturable survivors and VBNC cells were quantified in *P. aeruginosa* PAO1 biofilms, developed in ID-MHII and M9, after 24-h exposure to CFD, TOB, and CAZ at their respective MBECs, using a previously validated biofilm persistence model [40].

Neither 24-h biofilms nor untreated controls developed VBNC subpopulations, and initial culturable cell counts were similar across low-iron media. After antibiotic treatment, CFD showed lower bactericidal activity than the other drugs. Following CFD exposure, culturable survivors were higher than after TOB or CAZ treatment. TVC counts, including both culturable and VBNC subpopulations, remained closer to initial levels (Table S1), with VBNC cells representing a notable fraction of the population (Fig. 1).

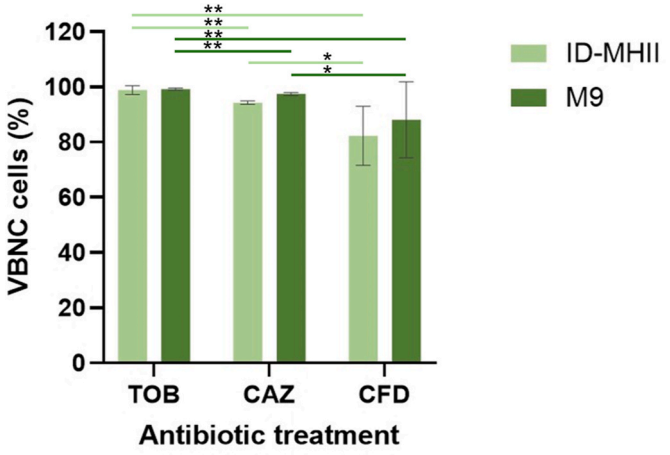

Fig. 1. *Pseudomonas aeruginosa* viable but non-culturable subpopulations in antibiotic-treated biofilms. *P. aeruginosa* PAO1 24-h biofilms developed in ID-MHII (light green bars) or M9 broth (dark green bars) were exposed for 24 h to tobramycin (TOB), ceftazidime (CAZ) or cefiderocol (CFD) at their Minimum Biofilm Eradication Concentration (MBEC). The number of culturable persisters and total viable cells was quantified by CFU counts and qPCR, respectively. The VBNC population was estimated as the difference between qPCR and CFU counts, and reported as a percentage of the total viable cells. Data are the average of three biological replicates of two independent experiments ±standard deviation. *: $p < 0.05$; **: $p < 0.01$. (For interpretation of the references to colour in this figure legend, the reader is referred to the Web version of this article.)

The non-culturable subpopulation of the biofilm was slightly more abundant in M9 than in ID-MHII; considering each antibiotic activity, TOB resulted in the main VBNC-inducing drug, in line with our previous investigations [16,40], followed by CAZ and CFD. This pattern was exhibited in both the low-iron media, indicating a lower though significant tendency of *P. aeruginosa* to enter the non-culturable state when exposed to CFD.

To further investigate the role of TOB, CAZ, and CFD in the induction of VBNC state at the single cell level, *P. aeruginosa* PAO1 biofilms grown in flow cells were exposed to eradicating concentrations (MBEC) of these three antibiotics and compared to the untreated biofilm (Fig. 2A and B).

TOB-, CAZ-, and CFD-treated biofilms showed a significant and remarkable reduction in biomass and thickness compared to untreated controls, in line with the results observed using the Calgary device (Fig. 2C). Although the membrane integrity of most cells dropped to barely detectable levels, residual respiratory activity and RNA content were still observed (Fig. 2D–G). The presence of membrane-damaged cells that retain basal respiratory and transcriptional activity, yet remain non-culturable (*i.e.*, undetectable when determining the MBEC), conformed to the characteristics of VBNC cells [41]. Interestingly, CAZ and CFD induced massive elongation in a subpopulation, increasing cell area and cell aspect ratio (length/width) (Fig. 3).

Filamentous cells displayed either separated nucleoids (red arrows, Fig. 3A) or diffused nucleic acids (cyan arrows, Fig. 3A), suggesting that septation of daughter cells did not occur in all elongated cells. Interestingly, the filamentous cell population showed a variable response to KK 1905 staining, which labels membrane-damaged cells (Fig. 3A), suggesting that cell filamentation does not contribute to CAZ or CFD tolerance, since both damaged and undamaged filamentous populations were observed.

3.4. *Efficacy of TOB and CFD in a murine model of P. aeruginosa chronic lung infection*

C57BL/6NCrlBR mice were challenged intratracheally with *P. aeruginosa* PAO1 strain embedded in agar beads to mimic chronic lung infection. Subcutaneous treatment with TOB 80 mg/kg and CFD 40 mg/kg was administered 24 h and 48 h post infection, to compare the *in vivo* efficacy of CFD-based therapy with the gold standard (*i.e.,* TOB-based therapy) of *P. aeruginosa* lung infection in CF. Mice treated with both TOB and CFD exhibited an initial weight loss at 24 h after infection. However, over the course of treatment, CFD-treated mice exhibited a faster recovery of body weight than the vehicle-treated mice (Fig. S3).

Compared to vehicle-treated mice, TOB-treated ones were able to reduce the *P. aeruginosa* bacterial burden in the lungs and in the BALF, with ~78% of the mice clearing the infection. Conversely, CFD-treated mice showed high variability in the response to this antibiotic, with almost 56% of mice clearing the infection. Consistent with the *in vitro* data, the induction of *P. aeruginosa* VBNC cells mirrored this pattern, with both TOB and CFD causing the entrance of the pathogen in the VBNC state in a higher percentage of animals, compared to the vehicle (88.90% and 77,80% vs 60%, for TOB-, CFD- and vehicle treated mice, respectively) (Fig. 4).

TOB and CFD treatments had no significant effect on pulmonary inflammation induced by chronic *P. aeruginosa* infection after 3 days of persistence; however, a positive trend in cell recruitment was observed (Fig. S4).

4. Discussion

CFD is a recently developed antimicrobial, currently adopted as a last-resort therapeutic option for difficult-to-treat infections unresponsive to the available antibiotic regimens. It is recommended against carbapenem-resistant *P. aeruginosa* [42], although the ability to endure CFD-exposure has been recently reported in this species [24].

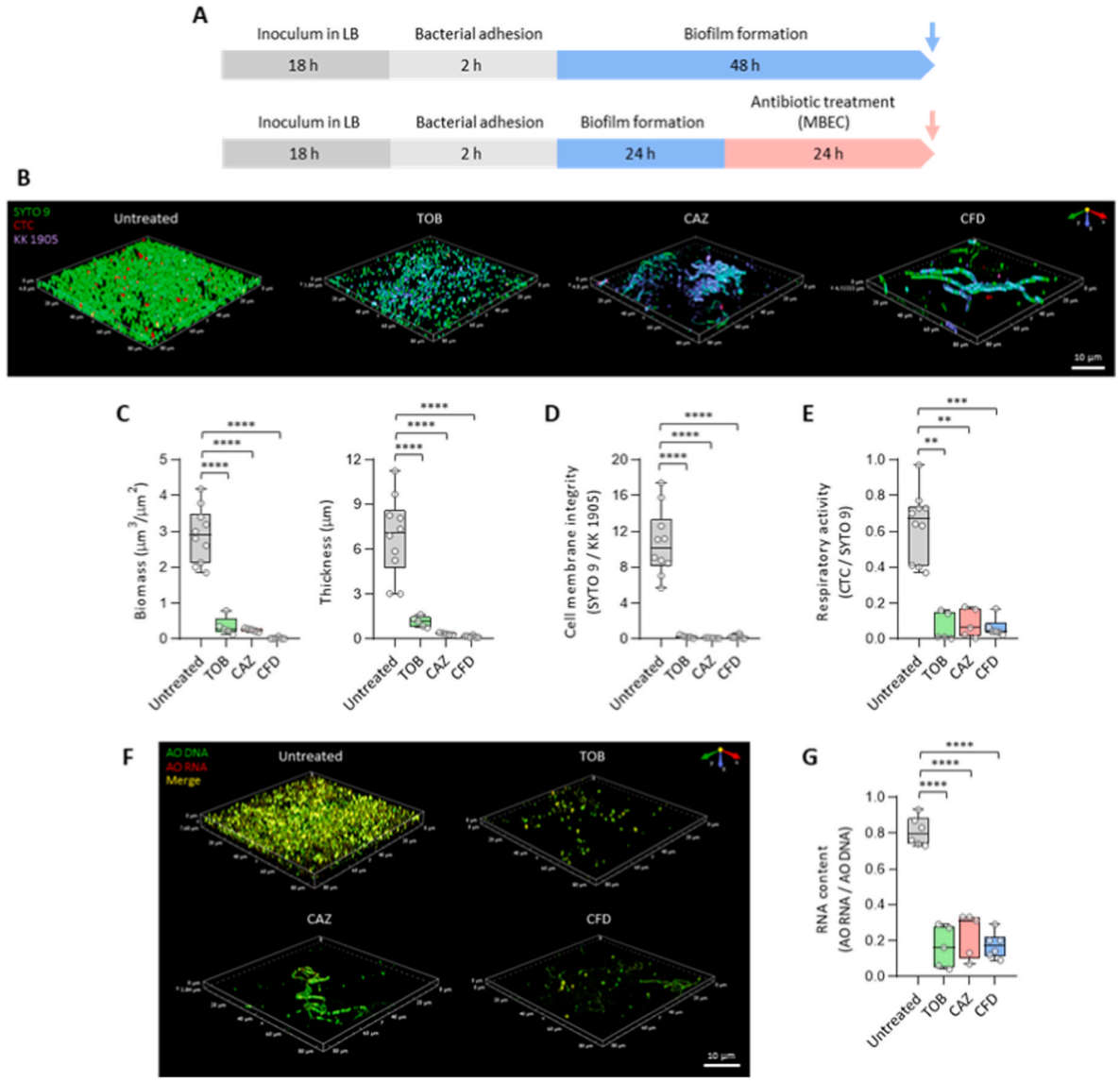

Fig. 2. Effects of TOB, CAZ, and CFD on *P. aeruginosa* PAO1 biofilm grown in flow cells. A, Schematic representation of the experimental timeline. Pink and cyan arrows indicate samples treated or not with MBEC of TOB, CFD, or CAZ, respectively. When indicated by arrows, biofilms were stained with a combination of SYTO 9, CTC, and KK 1905 or with AO. **B**, Representative 3D projections of SYTO 9 (green)-, CTC (red)-, and KK 1905 (purple)-merged channels of biofilms untreated or treated with the indicated antibiotics. **C**, Biofilm spatial characteristics determined by using the COMSTAT software from CLSM images. **D**, Cell membrane integrity assessed by calculating the ratio of biomass measured from SYTO 9 and KK 1905 channels in both untreated and antibiotic-treated biofilms. **E**, Respiratory activity expressed as the ratio of biomass measured from CTC and SYTO 9 channels in both untreated and antibiotic-treated biofilms. **F**, 3D projections displaying merged channels of DNA (green) and RNA (red) emissions for AO-stained biofilms from untreated and antibiotic-treated samples. **G**, RNA content of untreated and antibiotic-treated biofilms calculated as the ratio between the biomass of red and green channels, representing the AO emissions resulting from RNA and DNA binding, respectively. Separated channels of the 3D projections displayed in **B** and **F** are provided in Fig. S5 and S6. The limits of each box plot in **C**, **D**, **E**, and **G** represent the first and third quartiles, and the values outside the boxes represent the maximum and minimum values. *P* values (**$P \leq 0.01$; ***$P \leq 0.001$; ****$P \leq 0.0001$) were calculated using the unpaired *t*-test. (For interpretation of the references to colour in this figure legend, the reader is referred to the Web version of this article.)

We have previously demonstrated that *P. aeruginosa* is capable of surviving antibiotic pressure within the CF environment as a result of the development of persistent and VBNC cells [13,40]. Therefore, this study aimed to compare the persistence and the induction of the specialized VBNC phenotype in *P. aeruginosa* biofilms after exposure to the siderophore-cephalosporin CFD, compared with a typical anti-pseudomonal antibiotic (TOB) and a third-generation cephalosporin (CAZ). It is worth noting that both CFD and CAZ share the carboxy-propanoxymino group which promotes transport across the bacterial outer member, but only CFD contains the chlorocatechol residue which improves active transport across siderophore receptors [20].

The previously validated experimental setting for bacterial persistence in both planktonic and biofilm cultures [40] was successfully adapted to the iron depletion condition. Although exerting different effects on the growth and biofilm production of *P. aeruginosa* PAO1, ID-MHII and M9 did not result in relevant differences in both antibiotic susceptibility and persistence assays. Noteworthy, neither of the two media caused the insurgence of the VBNC phenotype in antibiotic-untreated biofilms, suggesting that iron depletion alone was not sufficient to promote the *P. aeruginosa* shift into the VBNC state.

Interestingly, CFD exhibited a slightly higher (2-fold MIC difference) antibacterial effect compared to TOB and CAZ in *P. aeruginosa* planktonic cultures. On the contrary, TOB showed lower MBEC values than CFD against *in vitro* biofilms. This pattern was observed even in both

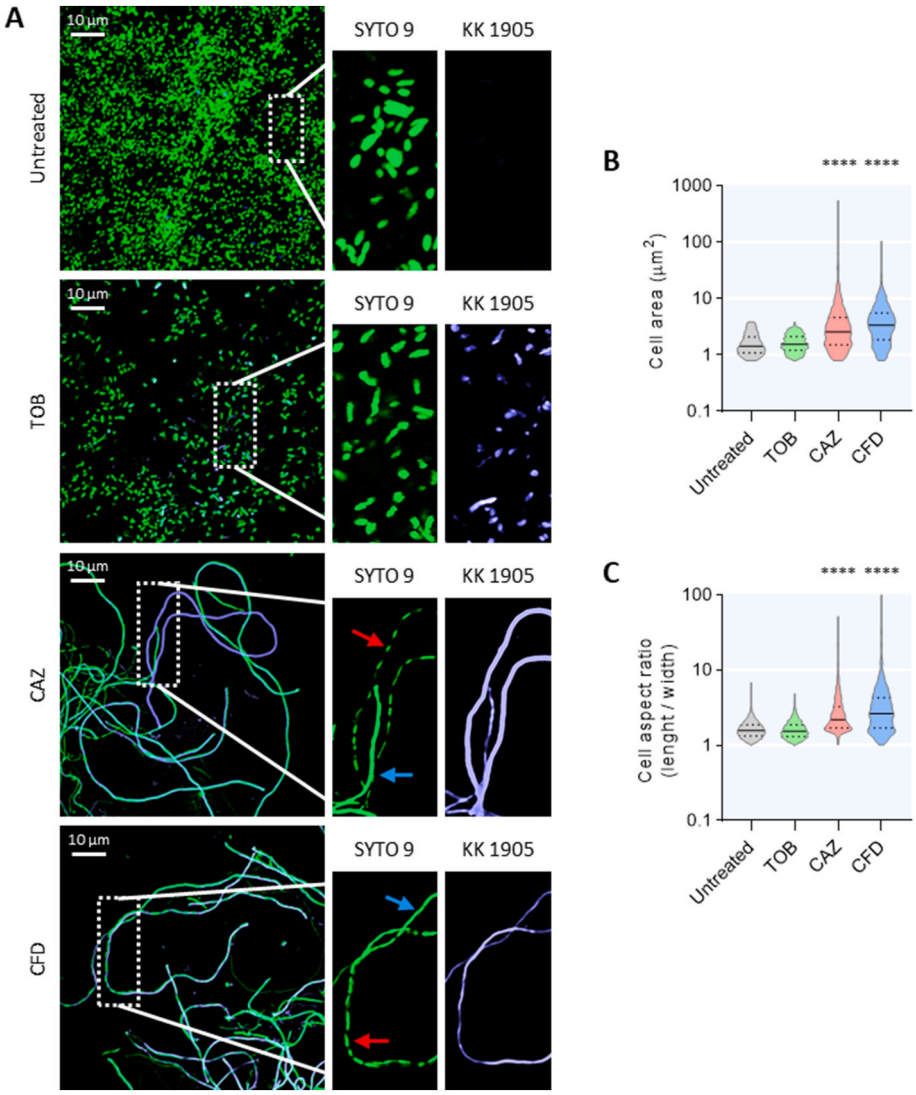

Fig. 3. CAZ and CFD induce *P. aeruginosa* cell filamentation. A, Representative maximum intensity projection images of *P. aeruginosa* PAO1 biofilms grown in flow cells, with and without treatment with MBECs of the indicated antibiotics. Biofilms were stained with a combination of SYTO 9 (green) and KK 1905 (purple). Dashed white rectangles highlight the areas where separate SYTO 9 and KK 1905 channels are displayed in the insets (right panels). Cyan and red arrows in the insets indicate cell filaments with diffused DNA and separated nucleoids, respectively. Violin plots showing cell area (**B**) and aspect ratio (**C**) calculated on CLSM images. *P* values (****$P \leq 0.0001$) were calculated using the unpaired *t*-test ($n > 1000$ cells for each condition). Asterisks indicate statistically significant differences compared to the untreated sample. (For interpretation of the references to colour in this figure legend, the reader is referred to the Web version of this article.)

planktonic and biofilm persistence assays, which showed a prominent role of TOB in reducing the amount of culturable *P. aeruginosa* survivors after antibiotic exposure. Remarkably, our results on CFU counts in CFD-exposed biofilms are in line with the results obtained by Ferretti et al. [43], where *P. aeruginosa* biofilms exposed to CFD 256 µg/ml showed an overall 1log CFU decrease, and with those by Fouad et al. [24], reporting between 4% and 61% CFD-persisters in cultures of different *P. aeruginosa* strains. In our assays, *P. aeruginosa* PAO1 planktonic cultures exhibited a survivor percentage of 37% in ID-MHII and 15% in M9 after 1-h exposure, while biofilm CFD-persisters accounted for 3.65% and 4.5% in ID-MHII and M9, respectively, after treatment with the antibiotic MBEC for 24h.

CFD-exposure resulted in a higher amount of culturable survivors in *P. aeruginosa* biofilms (around $9{,}67x10^4$ CFU/ml), compared to TOB-exposure (around $5{,}00x10^3$ CFU/ml), in contrast with the notion that aminoglycosides, mimicking the effect of toxin-antitoxin modules, are the strongest inducers of persisters [44].

Interestingly, the siderophore cephalosporin induced a lower shift of *P. aeruginosa* cells to the VBNC state (less than 90% of TVCs), if compared to CAZ (between 94% and 97.5%) or TOB (more than 98.5%), regardless of the culture medium. This might indicate that *P. aeruginosa* can easily tolerate the activity of CFD, without entering a deeply quiescent state, such as the non-culturable one. The active uptake of CFD by bacterial cells, due to the iron-binding ability of the antibiotic, might suggest an active metabolic state of most *P. aeruginosa* biofilm cells, not corresponding to the VBNC state, and justifying a higher recovery of culturable survivors. However, the present data do not allow hypothesizing specific adaptations strategies against CFD, which are currently under investigation.

Confocal microscopy revealed residual respiratory and transcriptional activity in non-culturable cells. Exposure to both CAZ and CFD induced the formation of *P. aeruginosa* filamentous forms. However, the involvement of these structures in the transition to the VBNC state remains debated, as they exhibited signs of membrane damage.

The therapeutic efficacy of the CFD treatment was then assessed in a pre-clinical murine *P. aeruginosa* lung infection model, which mirrored the results obtained *in vitro*. TOB-treated animals exhibited the highest infection clearance rate, yet also the greatest occurrence of VBNC cells.

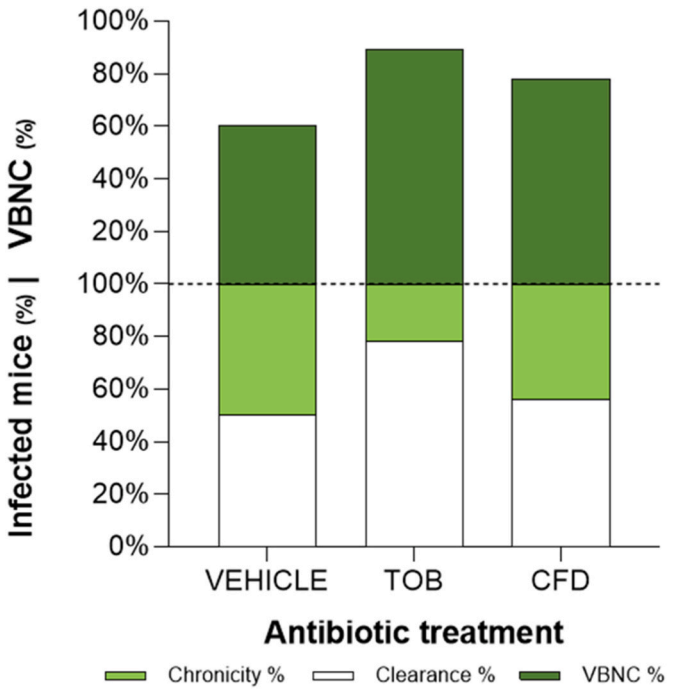

Fig. 4. *Pseudomonas aeruginosa* infection treatment in a pre-clinical mouse model. C57bl/6NCrlBR mice were infected with 1×10^6 colony-forming units (CFUs) of *P. aeruginosa* PAO1 strain embedded in agar beads by intratracheal administration and treated subcutaneously 24 h and 48 h after infection with saline (VEHICLE), tobramycin 80 mg/kg (TOB) or cefiderocol 40 mg/kg (CFD). 72 h post infection mice were sacrificed, and the total lung bacterial burden was quantified by plate count and qPCR analysis. The VBNC subpopulation was calculated as discrepancy between qPCR and CFU counts. The percentage of mice showing infection clearance (*i.e.,* $< 10^3$ total CFU by culture after antibiotic treatment, white bars) or chronic infection (*i.e.,* $\geq 10^3$ total CFU by culture, light green bars) and the presence of VBNC cells (dark green bars) was calculated for each scheduled treatment. Four-five mice for group (*i.e.,* treatment with VEHICLE, TOB, or CFD) were used in two independent experiments. (For interpretation of the references to colour in this figure legend, the reader is referred to the Web version of this article.)

CFD-treatment was responsible for the induction of VBNC cells in a higher number of animals compared to the vehicle, but did not match the effect exerted by TOB. We used male mice to minimize hormonal variability affecting host responses; future work should evaluate sex-related differences in disease progression and treatment response. CFD is known to require prolonged therapeutic coverage during infection treatment, achieved through repeated administration, to reach its full efficacy [45], which could explain the higher bacterial survival and the lower induction of VBNC cells. The consistency between *in vitro* and *in vivo* data suggests that CFD has a limited ability to induce dormancy in the pathogen. This may represent an advantage, as the course of infection could reliably be monitored using standard culture-based techniques, even after treatment completion.

Overall, the results obtained in this study confirmed the capability of *P. aeruginosa* to endure the treatment with CFD, which might impair the efficacy of antibiotic therapies based on this drug. Bacterial persistence is becoming an increasing health issue, although it is often overlooked compared with the problem of antibiotic resistance. The identification of CFD resistance determinants and their specific contribution to the resistance levels in *P. aeruginosa* has already been reported [46], while only limited information is available about the persistence-inducing activity of CFD, specifically in the development of VBNC subpopulations. The results obtained in this work contribute to fill this knowledge gap and provide novel information on the CFD efficacy against difficult-to-treat infections. They also warrant further studies about the persistence mechanisms, specifically the gene pathways regulating the bacterial response to CFD, and possible antibiotic combinatory or adjuvant strategies, to potentiate the CFD activity and achieve the infection clearance.

Funding

This work was supported by the Italian Cystic Fibrosis Research Foundation [grant number FFC#07/2023 to B.C. thanks the contributions of FFC Ricerca Delegations of Ferrara, Belluno, Cecina e Rosignano, Prato, Pavia, together with Amici della Ricerca and Adare Pharma Solutions] and by Fano Ateneo Association [B.C.]. The funders played no role in study design, data collection, analysis and interpretation of data, or the writing of this manuscript.

CRediT authorship contribution statement

Gianmarco Mangiaterra: Conceptualization, Data curation, Investigation, Methodology, Validation, Writing – original draft. **Massimiliano Lucidi:** Conceptualization, Data curation, Investigation, Methodology, Software, Validation, Writing – original draft. **Giorgia Piccioni:** Investigation, Writing – review & editing. **Riccardo Rosa:** Investigation, Writing – review & editing. **Davide Gugliandolo:** Formal analysis, Investigation, Software, Writing – review & editing. **Ida De Fino:** Formal analysis, Investigation, Writing – review & editing. **Martina Rossano:** Formal analysis, Investigation, Writing – review & editing. **Carla Vignaroli:** Data curation, Validation, Writing – review & editing. **Paolo Visca:** Data curation, Validation, Writing – review & editing. **Alessandra Bragonzi:** Conceptualization, Data curation, Methodology, Validation, Writing – original draft. **Barbara Citterio:** Conceptualization, Data curation, Funding acquisition, Methodology, Project administration, Supervision, Validation, Writing – review & editing.

Declaration of competing interest

The authors declare the following financial interests/personal relationships which may be considered as potential competing interests: Barbara Citterio reports financial support was provided by Italian Cystic Fibrosis Research Foundation. Barbara Citterio reports financial support was provided by Fano Ateneo Association. If there are other authors, they declare that they have no known competing financial interests or personal relationships that could have appeared to influence the work reported in this paper.

Acknowledgements

We thank Professor Emanuela Frangipani (University of Urbino) for providing the reference *P. aeruginosa* PAO1 strain and the engineered variant PAO1 P*pvdE::lux*.

Appendix A. Supplementary data

Supplementary data to this article can be found online at https://doi.org/10.1016/j.bioflm.2026.100370.

Data availability

Data used in the study are included in the manuscript and/or supporting information.

References

[1] Stover CK, Pham XQ, Erwin AL, Mizoguchi SD, Warrener P, Hickey MJ, Brinkman FS, Hufnagle WO, Kowalik DJ, Lagrou M, Garber RL, Goltry L, Tolentino E, Westbrock-Wadman S, Yuan Y, Brody LL, Coulter SN, Folger KR, Kas A, Larbig K, Lim R, Smith K, Spencer D, Wong GK, Wu Z, Paulsen IT, Reizer J,

Saier MH, Hancock RE, Lory S, Olson MV. Complete genome sequence of *Pseudomonas aeruginosa* PAO1, an opportunistic pathogen. Nature 2000;406:959–64. https://doi.org/10.1038/35023079.

[2] Botelho J, Tüffers L, Fuss J, Buchholz F, Utpatel C, Klockgether J, Niemann S, Tümmler B, Schulenburg H. Phylogroup-specific variation shapes the clustering of antimicrobial resistance genes and defence systems across regions of genome plasticity in *Pseudomonas aeruginosa*. EBioMedicine 2023;90:104532. https://doi.org/10.1016/j.ebiom.2023.104532.

[3] Weimann A, Dinan AM, Ruis C, Bernut A, Pont S, Brown K, Ryan J, Santos L, Ellison L, Ukor E, Pandurangan AP, Krokowski S, Blundell TL, Welch M, Blane B, Judge K, Bousfield R, Brown N, Bryant JM, Kukavica-Ibrulj I, Rampioni G, Leoni L, Harrison PT, Peacock SJ, Thomson NR, Gauthier J, Fothergill JL, Levesque RC, Parkhill J, Floto RA. Evolution and host-specific adaptation of *Pseudomonas aeruginosa*. Science 2024;385. https://doi.org/10.1126/science.adi0908. eadi0908.

[4] Fernández-Barat L, Ferrer M, De Rosa F, Gabarrús A, Esperatti M, Terraneo S, Rinaudo M, Li Bassi G, Torres A. Intensive care unit-acquired pneumonia due to *Pseudomonas aeruginosa* with and without multidrug resistance. J Infect 2017;74:142–52. https://doi.org/10.1016/j.jinf.2016.11.008.

[5] Casaredi IG, Shaw M, Waters V, Seeto R, Blanchard AC, Ratjen F. Impact of antibiotic eradication therapy of *Pseudomonas aeruginosa* on long term lung function in cystic fibrosis. J Cyst Fibros 2023;22:98–102. https://doi.org/10.1016/j.jcf.2022.08.007.

[6] Elborn JS. Cystic fibrosis. Lancet 2016;388:2519–31. https://doi.org/10.1016/S0140-6736(16)00576-6.

[7] Kunisch F, Campobasso C, Wagemans J, Yildirim S, Chan BK, Schaudinn C, Lavigne R, Turner PE, Raschke MJ, Trampuz A, Gonzalez Moreno M. Targeting *Pseudomonas aeruginosa* biofilm with an evolutionary trained bacteriophage cocktail exploiting phage resistance trade-offs. Nat Commun 2024;15:8572. https://doi.org/10.1038/s41467-024-52595-w.

[8] Allen L, Allen L, Carr SB, Davies G, Downey D, Egan M, Forton JT, Gray R, Haworth C, Horsley A, Smyth AR, Southern KW, Davies JC. Future therapies for cystic fibrosis. Nat Commun 2023;14:693. https://doi.org/10.1038/s41467-023-36244-2.

[9] Coenye T, Bové M, Bjarnsholt T. Biofilm antimicrobial susceptibility through an experimental evolutionary lens. npj Biofilms Microbiomes 2022;8:82. https://doi.org/10.1038/s41522-022-00346-4.

[10] Malhotra S, Hayes Jr D, Wozniak DJ. Mucoid *Pseudomonas aeruginosa* and regional inflammation in the cystic fibrosis lung. J Cyst Fibros 2019;18:796–803. https://doi.org/10.1016/j.jcf.2019.04.009.

[11] Balaban NQ, Helaine S, Lewis K, Ackermann M, Aldridge B, Andersson DI, Brynildsen MP, Bumann D, Camilli A, Collins JJ, Dehio C, Fortune S, Ghigo JM, Hardt WD, Harms A, Heinemann M, Hung DT, Jenal U, Levin BR, Michiels J, Storz G, Tan MW, Tenson T, Van Melderen L, Zinkernagel A. Definitions and guidelines for research on antibiotic persistence. Nat Rev Microbiol 2019;17:441–8. https://doi.org/10.1038/s41579-019-0196-3.

[12] Ayrapetyan M, Williams T, Oliver JD. Relationship between the viable but nonculturable state and antibiotic persister cells. J Bacteriol 2018;200. https://doi.org/10.1128/JB.00249-18. e00249–e00218.

[13] Cirilli N, Schiavoni V, Tagliabracci V, Gesuita R, Tiano L, Fabrizzi B, D'Antuono A, Peruzzi A, Cedraro N, Carle F, Moretti M, Ferrante L, Vignaroli C, Biavasco F, Mangiaterra G. Role of viable but non culturable cells in patients with cystic fibrosis in the era of highly effective modulator therapy. J Cyst Fibros 2024. https://doi.org/10.1016/j.jcf.2024.02.013. S1569–19932400026–2.

[14] Mangiaterra G, Amiri M, Di Cesare A, Pasquaroli S, Manso E, Cirilli N, Citterio B, Vignaroli C, Biavasco F. Detection of viable but non-culturable *Pseudomonas aeruginosa* in cystic fibrosis by qPCR: a validation study. BMC Infect Dis 2018;18:701. https://doi.org/10.1186/s12879-018-3612-9.

[15] Stanojevic S, Waters V, Mathew JL, Taylor L, Ratjen F. Effectiveness of inhaled tobramycin in eradicating *Pseudomonas aeruginosa* in children with cystic fibrosis. J Cyst Fibros 2014;13:172–8. https://doi.org/10.1016/j.jcf.2013.09.002.

[16] Mangiaterra G, Cedraro N, Vaiasicca S, Citterio B, Frangipani E, Biavasco F, Vignaroli C. Involvement of acquired tobramycin resistance in the shift to the viable but non-culturable state in *Pseudomonas aeruginosa*. Int J Mol Sci 2023;24:11618. https://doi.org/10.3390/ijms241411618.

[17] Bassetti M, Echols R, Matsunaga Y, Ariyasu M, Doi Y, Ferrer R, Lodise TP, Naas T, Niki Y, Paterson DL, Portsmouth S, Torre-Cisneros J, Toyoizumi K, Wunderink RG, Nagata TD. Efficacy and safety of cefiderocol or best available therapy for the treatment of serious infections caused by carbapenem-resistant Gram-negative bacteria (CREDIBLE-CR): a randomised, open-label, multicentre, pathogen-focused, descriptive, phase 3 trial. Lancet Infect Dis 2021;21:226–40. https://doi.org/10.1016/S1473-3099(20)30796-9.

[18] Ito A, Nishikawa T, Matsumoto S, Yoshizawa H, Sato T, Nakamura R, Tsuji M, Yamano Y. Siderophore cephalosporin cefiderocol utilizes ferric iron transporter systems for antibacterial activity against *Pseudomonas aeruginosa*. Antimicrob Agents Chemother 2016;60:7396–401. https://doi.org/10.1128/AAC.01405-16.

[19] Holbein BE, Ang MTC, Allan DS, Chen W, Lehmann C. Iron-withdrawing anti-infectives for new host-directed therapies based on iron dependence, the Achilles' heel of antibiotic-resistant microbes. Environ Chem Lett 2021;9:2789–808. https://doi.org/10.1007/s10311-021-01242-7.

[20] Sato T, Yamawaki K. Cefiderocol: discovery, chemistry, and *in vivo* profiles of a novel siderophore cephalosporin. Clin Infect Dis 2019;69:S538–43. https://doi.org/10.1093/cid/ciz826.

[21] López-Causapé C, Maruri-Aransolo A, Gomis-Font MA, Penev I, Castillo MG, Mulet X, de Dios Caballero J, Campo RD, Cantón R, Oliver A. Cefiderocol resistance genomics in sequential chronic *Pseudomonas aeruginosa* isolates from cystic fibrosis patients. Clin Microbiol Infect 2023;29. https://doi.org/10.1016/j.cmi.2022.11.014. 538.e7-538.e13.

[22] Maruri-Aransolo A, López-Causapé C, Hernández-García M, García-Castillo M, Caballero-Pérez JD, Oliver A, Cantón R. *In vitro* activity of cefiderocol in *Pseudomonas aeruginosa* isolates from people with cystic fibrosis recovered during three multicentre studies in Spain. J Antimicrob Chemother 2024;79:1432–40. https://doi.org/10.1093/jac/dkae126.

[23] Fabrizio G, Truglio M, Cavallo I, Sivori F, Francalancia M, Cabral RJR, Comar M, Trancassini M, Compagnino DE, Diaco F, Antonelli G, Ascenzioni F, Cimino G, Pimpinelli F, Di Domenico EG. Cefiderocol activity against planktonic and biofilm forms of β-lactamase-producing *Pseudomonas aeruginosa* from people with cystic fibrosis. J Glob Antimicrob Resist 2025;28. https://doi.org/10.1016/j.jgar.2025.04.010. S2213-7165(25)00082-7.

[24] Fouad A, Nicolau SE, Tamma PD, Simner PJ, Nicolau DP, Gillet CM. Differential frequency of persister cells in clinically derived isolates of *Pseudomonas aeruginosa* after exposure to cefiderocol and ceftolozane/tazobactam. J Antimicrob Chemother 2024;79:3236–42. https://doi.org/10.1093/jac/dkae346.

[25] Imperi F, Massai F, Facchini M, Frangipani E, Visaggio D, Leoni L, Bragonzi A, Visca P. Repurposing the antimycotic drug flucytosine for suppression of *Pseudomonas aeruginosa* pathogenicity. Proc Natl Acad Sci USA 2013;110:7458–63. https://doi.org/10.1073/pnas.1222706110.

[26] Clinical and Laboratory Standards Institute. Performance standards for antimicrobial susceptibility testing: twenty-seventh informational supplement M100-S27. Wayne, PA, USA: CLSI; 2020.

[27] Revest M, Jacqueline C, Boudjemaa R. New *in vitro* and *in vivo* models to evaluate antibiotic efficacy in *Staphylococcus aureus* prosthetic vascular graft infection. J Antimicrob Chemother 2016;71:1291–9. https://doi.org/10.1093/jac/dkv496.

[28] Mellini M, Lucidi M, Imperi F, Visca P, Leoni L, Rampioni G. Generation of genetic tools for gauging multiple-gene expression at the single-cell level. Appl Environ Microbiol 2021;87. https://doi.org/10.1128/AEM.02956-20. e02956-20.

[29] Lucidi M, Capecchi G, Visaggio D, Gasperi T, Parisi M, Cincotti G, Rampioni G, Visca P, Kolmakov K. Expanding the microbiologist toolbox via new far-red-emitting dyes suitable for bacterial imaging. Microbiol Spectr 2024;12:e0369023. https://doi.org/10.1128/spectrum.03690-23.

[30] Créach V, Baudoux AC, Bertru G, Rouzic BL. Direct estimate of active bacteria: CTC use and limitations. J Microbiol Methods 2003;52:19–28. https://doi.org/10.1016/s0167-7012(02)00128-8.

[31] Stiefel P, Rosenberg U, Schneider J, Mauerhofer S, Maniura-Weber K, Ren Q. Is biofilm removal properly assessed? Comparison of different quantification methods in a 96-well plate system. Appl Microbiol Biotechnol 2016;100:4135–45. https://doi.org/10.1007/s00253-016-7396-9.

[32] Lucidi M, Imperi F, Artuso I, Capecchi G, Spagnoli C, Visaggio D, Rampioni G, Leoni L, Visca P. Phage-mediated colistin resistance in *Acinetobacter baumannii*. Drug Resist Updates 2024;73:101061. https://doi.org/10.1016/j.drup.2024.101061.

[33] Plemel JR, Caprariello AV, Keough MB, Henry TJ, Tsutsui S, Chu TH, Schenk GJ, Klaver R, Yong VW, Stys PK. Unique spectral signatures of the nucleic acid dye acridine orange can distinguish cell death by apoptosis and necroptosis. J Cell Biol 2017;216:1163–81. https://doi.org/10.1083/jcb.201602028.

[34] Sposato D, Mercolino J, Torrini L, Sperandeo P, Lucidi M, Alegiani R, Varone I, Molesini G, Leoni L, Rampioni G, Visca P, Imperi F. Redundant essentiality of AsmA-like proteins in *Pseudomonas aeruginosa*. mSphere 2024;9:e0067723. https://doi.org/10.1128/msphere.00677-23.

[35] Bragonzi A. Murine models of acute and chronic lung infection with cystic fibrosis pathogens. Int J Med Microbiol 2010;300:584–93. https://doi.org/10.1016/j.ijmm.2010.08.012.

[36] Cigana C, Ranucci S, Rossi A, De Fino I, Melessike M, Bragonzi A. Antibiotic efficacy varies based on the infection model and treatment regimen for *Pseudomonas aeruginosa*. Eur Respir J 2020;55:1802456. https://doi.org/10.1183/13993003.02456-2018.

[37] Facchini M, De Fino I, Riva C, Bragonzi A. Long term chronic *Pseudomonas aeruginosa* airway infection in mice. J Vis Exp 2014;85:51019. https://doi.org/10.3791/51019.

[38] Kukavica-Ibrulj I, Facchini M, Cigana C, Levesque RC, Bragonzi A. Assessing *Pseudomonas aeruginosa* virulence and the host response using murine models of acute and chronic lung infection. Methods Mol Biol 2014;1149:757–71. https://doi.org/10.1007/978-1-4939-0473-0_58.

[39] Bragonzi A, Paroni M, Nonis A, Cramer N, Montanari S, Rejman J, Di Serio C, Döring G, Tümmler B. *Pseudomonas aeruginosa* microevolution during cystic fibrosis lung infection establishes clones with adapted virulence. Am J Respir Crit Care Med 2009;180:138–45. https://doi.org/10.1164/rccm.200812-1943OC.

[40] Mangiaterra G, Carotti E, Vaiasicca S, Cedraro N, Citterio B, La Teana A, Biavasco F. Contribution of drugs interfering with protein and cell wall synthesis to the persistence of *Pseudomonas aeruginosa* biofilms: an in vitro model. Int J Mol Sci 2021;22:1628. https://doi.org/10.3390/ijms22041628.

[41] Liu J, Yang L, Kjellerup BV, Xu Z. Viable but nonculturable (VBNC) state, an underestimated and controversial microbial survival strategy. Trends Microbiol 2023;31:1013–23. https://doi.org/10.1016/j.tim.2023.04.009.

[42] Doi Y. Treatment options for carbapenem-resistant gram-negative bacterial infections. Clin Infect Dis 2019;69:S565–75. https://doi.org/10.1093/cid/ciz830.

[43] Ferretti C, Poma NV, Bernardo M, Rindi L, Cesta N, Tavanti A, Tascini C, Di Luca M. Evaluation of antibiofilm activity of cefiderocol alone and in combination with imipenem against *Pseudomonas aeruginosa*. J Glob Antimicrob Resist 2024;37:53–61. https://doi.org/10.1016/j.jgar.2024.01.021.

[44] Michiels JE, Van den Bergh B, Verstraeten N, Fauvart M, Michiels J. *In vitro* emergence of high persistence upon periodic aminoglycoside challenge in the

ESKAPE pathogens. Antimicrob Agents Chemother 2016;60:4630–7. https://doi.org/10.1128/AAC.00757-16.

[45] Matsumoto S, Singley CM, Hoover J, Nakamura R, Echols R, Rittenhouse S, Tsuji M, Yamano Y. Efficacy of cefiderocol against carbapenem-resistant gram-negative Bacilli in immunocompetent-rat respiratory tract infection models recreating human plasma pharmacokinetics. Antimicrob Agents Chemother 2017; 61:e00700–17. https://doi.org/10.1128/AAC.00700-17.

[46] González-Pinto L, Blanco-Martín T, Alonso-García I, Rodríguez-Pallares S, Outeda-García M, Gomis-Font MA, Fraile-Ribot PA, Vázquez-Ucha JC, González-Bello C, Beceiro A, Oliver A, Bou G, Arca-Suárez J. Impact of transferable betalactamases and intrinsic AmpC amino acid substitutions on the activity of cefiderocol against wildtype and iron uptake-deficient mutants of *Pseudomonas aeruginosa*. J Antimicrob Chemother 2024;17. https://doi.org/10.1093/jac/dkae326. dkae326.